



## Experimental and Numerical Investigation of Second Mode of Failure in Unlike End Notch Flexure Samples

S. Maleki, A. Andakhshideh\*, A. Seyfi

Department of Mechanical Engineering, Quchan University of Technology, Quchan, Iran

**ABSTRACT:** Localized lamination using composites is one of the effective solutions to repair damaged metallic pipelines. The connection of composite repair to the metal substructure in this method is one of the most important design parameters. Therefore, deriving the important parameters at the junction will help engineers in designing and predicting the interlaminar crack initiation and propagation at the composite/metal interface. In this paper, to investigate the second mode of failure in this method, the strain energy release rate is calculated experimentally and numerically in a steel/composite bond. According to an experimental standard for calculating the second mode strain energy release rate, ASTM-D7905, experimental tests are accomplished for three symmetric and asymmetric unlike end-notched flexure specimens and a relationship for the thickness of each material to have symmetric specimens is proposed. To validate the thickness calculation relationship, the finite element modeling of unlike samples using virtual crack closure technique is used which indicates the good agreement of experimental and numerical results. Comparing the experimental results showed that the strain energy release rate of symmetric samples is more than asymmetric ones and about 1.6 times as large.

### Review History:

Received: 2018/11/17

Revised: 2019/02/04

Accepted: 2019/03/11

Available Online: 2019/03/18

### Keywords:

Crack propagation

Second mode of failure

Strain energy release rate

Virtual crack closure technique

Unlike end-notched flexure specimen

### 1- Introduction

There are over 1.1 million miles of gas, petroleum, and crude oil pipelines worldwide. The corrosion of these pipelines is a significant problem, impacting both the operational safety and the economics of the pipeline. The repair methods based on bonded composite materials have recently gained popularity [1]. The connection of composite repair to the metal substructure is one of the most important design parameters. Investigating the delamination toughness and strain energy release rate of failure in the metal/composite interface can help designers in this regard. The Virtual Crack Closure Technique (VCCT) is widely used to compute the energy release rate,  $G$ , in the finite element analysis of fracture mechanics problems [2].

Moura et al. [3] proposed a new data reduction scheme for measuring the critical fracture energy of adhesive joints under pure mode II loading using the End Notched Flexure (ENF) test. The method was based on the crack equivalent concept and did not require crack length monitoring during propagation. Mollón et al. [4] carried out pure modes I and II and mixed-mode ratio tests, respectively by means of the following methods: Double Cantilever Beam (DCB), End Notch Flexure (ENF), and Asymmetric Double Cantilever Beam (ADCB). In Mollón et al. [4] the Finite Element Method (FEM) was used to analyze the stress state ahead of the crack to better explain the fracture micromechanisms

\*Corresponding author's email: a.andakhshideh@qiet.ac.ir

acting under different loading modes and their influence on delamination fracture toughness.

In this paper, the interlaminar strain energy release rate is calculated experimentally and numerically in a steel/composite bond. ASTM-D7905 [5], is an experimental standard for calculating the strain energy release rate in the second mode of failure for symmetric end-notched flexure specimens. In this paper, due to the unlike of the upper and lower beams, first, the relationships for the thickness calculation of composite and steel beams to have symmetric samples is obtained and experimental tests are carried out. Next, the finite element modeling of unlike samples using virtual crack closure method is applied to validate thickness calculation relationship which indicates its accuracy.

### 2- Experimental Procedure

#### 2- 1- The thickness of steel and composite beams in unlike end-notched flexure specimen

To find relationships for thickness ratio of steel and composite, the curvature radius of beams is assumed to be equal. We have,

$$\frac{h_{comp}}{h_{st}} = \sqrt[3]{\frac{E_{st}(1-\nu_{21}\nu_{12})E_2}{E_1E_2 - \nu_{12}^2E_2^2}} \quad (1)$$

Where,  $h_{comp}$  is composite thickness,  $h_{st}$ , steel thickness,  $E_{st}$ , elasticity module of steel,  $E_1, E_2$ , elasticity module of

composite in 1,2 directions and  $\nu_{21}, \nu_{12}$  are possession ratios of the composite.

2- 2- 2.2. Sample fabrication

Samples are unidirectional glass fiber epoxy composite/ steel. In composite section, 6 and 8 layers are used in symmetric Unlike End-Notched Flexure (UENF) specimens and Asymmetric Unlike End-Notched Flexure (AUENF) specimens, respectively. Steel ( $E = 208 \text{ GPa}, \nu = 0.3$ ) thickness is 2 mm and composite thickness is calculated using Eq. (1) for UENF samples and is equal to 3 mm in AUENF samples (Fig. 1). Three symmetric and asymmetric samples in similar laboratory conditions and the same material are made to increase test result precision. Mechanical properties of composite beams are listed in Table 1.

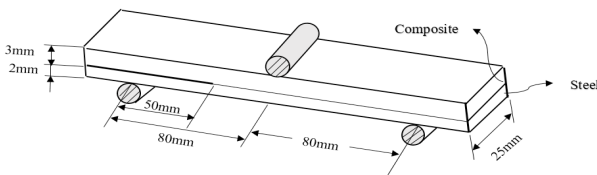


Fig. 1. AUENF schematic

Table 1. Mechanical properties of composite (Unidirectional glass fiber /epoxy resin) [6]

$E_1$ (GPa)	$E_2$ (GPa)	$E_3$ (GPa)	$\nu_{12} = \nu_{23}$ $= \nu_{13}$	$G_{12} = G_{13} =$ $G_{23}$ (GPa)
30	3	2	0.3	4

2- 3- Test procedure

Three-point bending test of end notch flexure samples are conducted according to ASTM-D7905. Quasi-static mode II tests were performed under the displacement control condition. The crosshead speed was set at 1.6 mm/min to ensure steady crack propagation and easy data recording. All tests are performed at 25oC and initial crack length, a, is 50 mm. A ZWICK/Z250 testing machine was used to conduct the ENF tests. A high precise load cell with a capacity of 50kg was utilized to record the load. The force–displacement ( $P-\delta$ ) curve, was recorded by the tensile machine. Both delamination length and local crack opening displacement in simultaneous with P and  $\delta$  during the test was recorded using a Canon EOS 100D camera.

2- 4- Data reduction for the experimental tests

2- 4- 1- Compliance Calibration Method (CCM)

As suggested in standard ASTM-D7905, the CCM can be used to determine  $G_{II}$  experimentally as:

$$G_{II} = \frac{P^2}{2b} \frac{dC}{da} \quad (2)$$

In Eq. (2),  $C = \delta / P$ , P and  $\delta$  are the load and load line deflection respectively. In addition, b is beam width and a is crack length. Assuming  $C = A + ma^3$  leads to:

$$G_{II} = \frac{3mP^2a^2}{2b} \quad (3)$$

In Eq. (3), m is the slope of C-a3 curve. This relation can be used to determine  $G_{II}$  in UENF [5] and AUENF [4].

2- 4- 2- 2.4.2. Direct Beam Theory (DBT)

In this method,  $G_{II}$  in UENF is calculated as [7-8],

$$G_{II} = \frac{P^2}{2b} \frac{dC}{da} = \frac{9P^2a^2}{8b^2 \left( \bar{Q}_{11}h_{Composite}^3 + E_{Steel}h_{Steel}^3 \right)} \quad (4)$$

2- 4- 3- Virtual crack closure technique

In 2D VCCT, the mode I, II components of the strain energy release rate,  $G_I$  and  $G_{II}$  are calculated for four noded elements as [2]:

$$G_I = \frac{1}{2b\Delta a} F_y (v_{comp} - v_{st}) \quad (5)$$

$$G_{II} = \frac{1}{2b\Delta a} F_x (u_{comp} - u_{st}) \quad (6)$$

where  $\Delta a$  is the length of the elements at the crack front and  $F_x, F_y$  are the forces at the crack tip. The relative displacements behind the crack tip are calculated from the nodal displacements at the upper crack face  $u_{comp}, v_{comp}$  and the nodal displacements  $u_{st}, v_{st}$  at the lower crack face, respectively [2].

3- Results and Discussion

In order to calculate the experimental strain energy release rate, the force-displacement curves of the symmetric and asymmetric unlike end notched flexure specimens are illustrated in Figs. 2 and 3, respectively. Next, using the data reduction schemes presented in the previous section, R-curve of UENF and AUENF samples are plotted in Figs. 4, 5, respectively. Crack growth path of unlike composite/steel ENF sample is shown in Fig. 6. It is seen in Fig. 6 that the crack propagation is occurred in the interface of composite/ steel and is not penetrated in composite or steel beams. The values of experimental and numerical (VCCT) strain energy release rate of unlike composite/steel ENF samples are listed in Table 3. Good agreement between experimental and numerical results are achieved which shows the validity of Eq. (1) for thickness ratio calculation of unlike materials in ENF tests to have symmetric samples.

4- Conclusion

In this paper, the experimental strain energy release rate of unlike symmetric and asymmetric composite/steel ENF samples was studied. To obtain symmetric unlike ENF samples, new relation (Eq. (1)) was suggested for steel and composite beams thicknesses in pure mode II experimental tests. Comparing the final experimental and numerical (VCCT) results shows that using Eq. (1) leads to the pure second mode of failure in unlike samples with 98% accuracy and can be used for further similar studies.

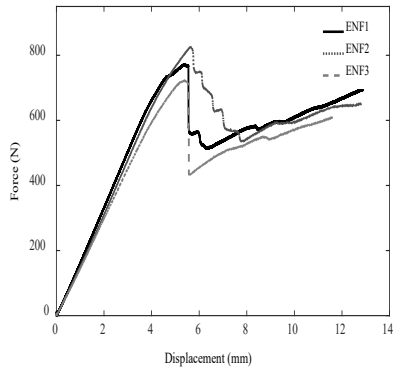


**Fig. 2 Experimental force-displacement curves of the UENF specimens**

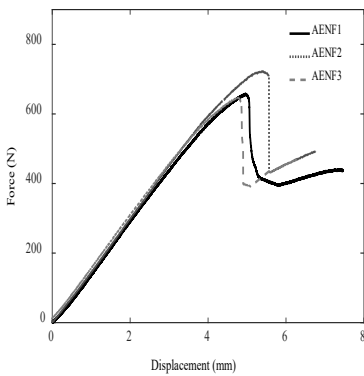


**Fig. 3 Experimental force-displacement curves of the AUENF specimens**

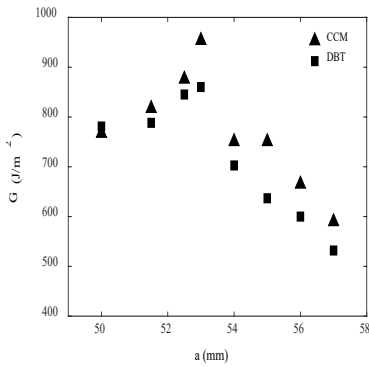


**Fig. 4 Experimental R-Curve of the UENF specimen**

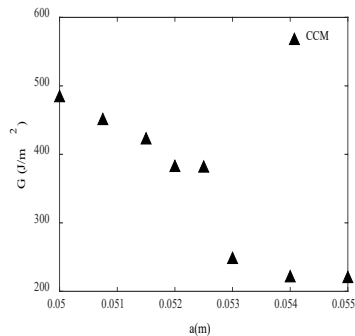


**Fig. 5 Experimental R-Curve of the AUENF specimen**

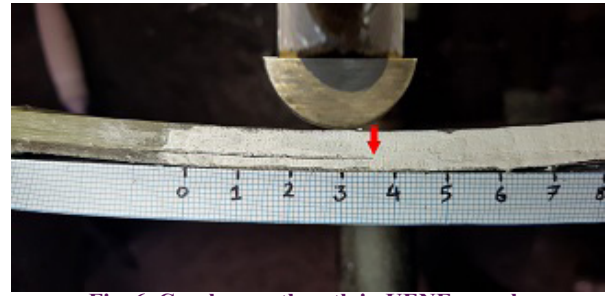


**Fig. 6. Crack growth path in UENF sample**

**Table 3. The values of the strain energy release rate of UENF samples**

	$G_{exp(DBT)}$	$G_{exp(CCM)}$	$G_{vcct}$	$G_{Ivcct}$	$G_{IIvcct}$
UENF	770.88	767.27	781.37	11.11	770.26
AUENF	--	482.4	480.62	144.21	336.41

**5- References**

[1] J.R. McCready, M. Knofczynski, M.W. Keller, Survivability of composite repairs of piping subjected to flexural loads, *International Journal of Pressure Vessels and Piping*, 152 (2017) 7-14.

[2] R. Krueger, Virtual crack closure technique: history, approach, and applications, *Applied Mechanics Reviews*, 57(2) (2004) 109-143.

[3] M. F. S. F. De Moura, R. D. S. G. Campilho, J. P. M. Gonçalves, Pure mode II fracture characterization of composite bonded joints, *International Journal of Solids and Structures*, 46(6) (2009) 1589-1595.

[4] V. Mollón, J. Bonhomme, A. Argüelles, J. Viña, Influence of the crack plane asymmetry over GII results in carbon epoxy ENF specimens, *Composite Structures*, 94(3) (2012) 1187-1191.

[5] ASTM, D7905/D7905M: Standard test method for mode II interlaminar fracture toughness of unidirectional fiber-reinforced polymer matrix composites, *American Standard of Testing Methods*, Vol. 4, pp. 1-18, 2014. doi: 10.1520/D7905\_D7905M-14.

[6] A. Kariman Moghadam, S. Rahnema, S. Maleki, Experimental and numerical investigation of crack growth in adhesive bonding of two composites plates under mode I, *Modares Mechanical Engineering*, 16(5) (2016) 271-280. (in Persian)

[7] W.S. Kim, J.J. Lee, Fracture characterization of interfacial cracks with frictional contact of the crack surfaces to predict failures in adhesive-bonded joints, *Engineering Fracture Mechanics*, 76 (2009) 1785-1799.

[8] F. Asgari Mehrabadi, *Fracture Mechanic Analysis In Adhesive Composite/Aluminum Joints*, MSc Thesis, University of Tabriz, Mechanical Engineering Department, September 2011.

